NSRRC - J0 04978 (>2015)

ADVANCED MATERIALS
www.advmat.de

Materials Views
www.MaterialsViews.com

Visible-Light Modulation on Lattice Dielectric Responses of a Piezo-Phototronic Soft Material

E-Wen Huang, Yu-Hsiang Hsu, Wei-Tsung Chuang, Wen-Ching Ko, Chung-Kai Chang, Chih-Kung Lee, Wen-Chi Chang, Tzu-Kang Liao, and Hao Cheng Thong*

The fundamental principle of piezo-phototronics was first introduced by Wang and co-workers in 2010.[1] They revealed a new perspective in semiconductors and opto-electronics by disclosing the piezo-phototronic effect, in which the piezopotential can be used to modulate the carrier activity and adjust the performance of optoelectronic devices. The sensitivity[2] and light emission[3] in piezo-phototronics have greatly improved by the advancement of nanotechnology, such as for example in ZnO, GaN, and InN in the wurtzite structure. Furthermore, piezoelectricity, which was traditionally encountered in single crystals, ceramics, or metal matrix composites,[4] has now also been documented for a number of polymers due to the need for flexibility. To apply the concept of piezo-phototronics reversely, Shih et al. have introduced the concept of photo-sensitive carrier activities, i.e., the optoelectronics, for tuning the piezoelectric properties of piezotronic devices via the bulk piezopotential.[5] Hence, polymer-based piezo-phototronics could potentially enable new applications in wearable electronics and many other flexible electronics.[6]

In recent years, piezoelectric polymers, such as poly(vinylidene fluoride) (PVDF)[7] and copolymers of vinylidene fluoride (VDF),[8,9] have attracted much attention because of their unique ferroelectric properties and broad application range combined with their flexibility. Their application and use in non-volatile memories, microelectronics, electromechanical applications, sensors and actuators have greatly increased in recent years.[9] This is due to the fact that piezoelectric polymers are relatively easier to fabricate in comparison to their counterparts. Piezoelectric polymers can also be molded and shaped more economically. Moreover, the flexibility of the polymer materials enables application on more portable electronics and tactile sensors.[10,11]

However, the integration of piezoelectricity, photonic excitation, and semiconductor transport for three-way coupling into soft materials is still in its early stages. It is not trivial to adjust and control the electro-optical properties between the coupled fields, which interplay with the strain-induced piezopotential. To obtain a better understanding of the piezo-phototronics for this class of soft materials, we have designed an in situ X-ray experiment to study the piezo-phototronic effect on piezoelectric P(VDF–TrFE) (poly(vinylidene fluoride-co-trifluoroethylene)) blended with photoconductive TiOPc (titanium oxide phthalocyanine) nanoparticles. This is a new class of piezo-phototronic composite that has been reported previously.[6,12] This composite not only has good piezoelectric properties but also shows high sensitivity to visible light. The X-ray diffraction spectrum was used to study its molecular information at lattice level. The experimental results of in situ X-ray were compared with the performance in bulk materials. The mechanical strain and microstructure at lattice level were investigated to disclose a three-way-coupled piezo-phototronic effect. The piezoelectric properties of this blended soft hybrid were further studied and compared with and without light illumination.

PVDF has four different phases, namely α, β, γ, and δ,[13,14] of which the configurations of the β-phase and α-phase are the most popular and well known.[11,14,15] The β-phase has an all-trains (TTTT) conformation of the polar phase and exhibits the highest piezoelectric response for this type of polymers because the dipoles are all aligned in the same direction.[16] In contrast, the α-phase is the most common polymorph of PVDF, which can easily be obtained through melting crystallization. The structure and phase transition of the copolymer crystals mainly depend on the TrFE content in the PVDF molecules and their copolymers.[17] Studies of the bulk average tensors for this type of polymers have been reported,[18] but its lattice tensors have not been measured directly yet.

Hence, the objectives of the present study are to: (i) characterize the lattice-level responses that are subjected to three-way piezo-phototronic controls; (ii) examine the behavior of the coexisting P(VDF–TrFE) matrix and TiOPc nanoparticles simultaneously; (iii) compare the responses of the bulk piezo-phototronic effect to the lattice structural evolution at different length

Prof. E.-W. Huang, H. C. Thong
Department of Materials Science and Engineering
National Chiao Tung University
1001 University Road
Hsinchu, Taiwan 30010, Taiwan (R.O.C.)
E-mail: ewenhuang@nctu.edu.tw
Prof. Y.-H. Hsu, Prof. C.-K. Lee, Dr. W.-C. Chang
Institute of Applied Mechanics
National Taiwan University
1, Sec. 4, Roosevelt Road
Taipei 106, Taiwan (R.O.C.)
Dr. W.-T. Chuang, C.-K. Chang
National Synchrotron Radiation Center
101, Hsin-Ann Road, Hsinchu Science Park
Hsinchu 30076, Taiwan (R.O.C.)
Dr. W.-C. Ko
Green Energy and Eco-Technology System Center
Industrial Technology Research Institute
ITRI Southern Campus
Tainan City 70955, Taiwan (R.O.C.)
T.-K. Liao
Department of Chemical and Materials Engineering
National Central University
No. 300, Zhongda Rd., Zhongli District
Taoyuan City 32001, Taiwan (R.O.C.)

DOI: 10.1002/adma.201503325

© 2015 WILEY-VCH Verlag GmbH & Co. KGaA, Weinheim

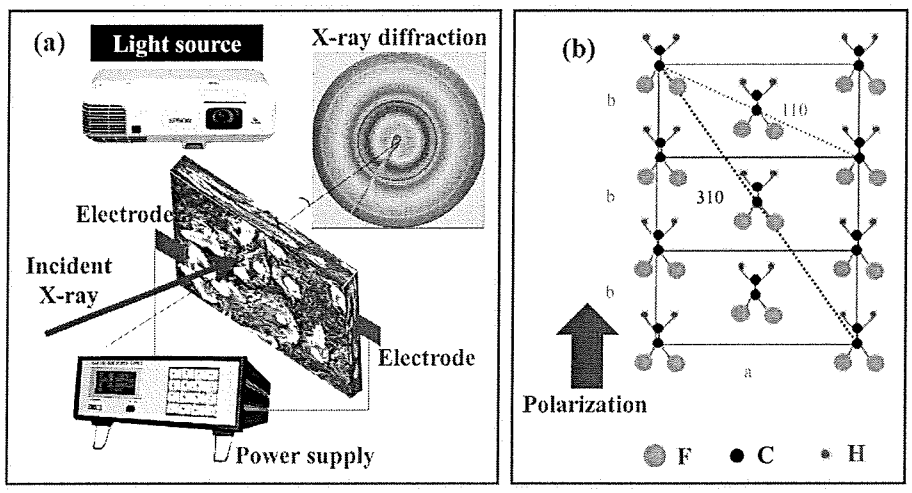

Figure 1. a) In situ synchrotron X-ray diffraction measurements. b) The lattice of the piezoelectric P(VDF–TrFE) matrix.

scales; and (iv) evaluate the underlying physical parameters, such as the dielectric properties, microscopically.

The setup of the X-ray diffraction measurement is shown in **Figure 1**a. This experimental configuration was designed to enable simultaneous determination of the ensemble-averaged crystalline phase responses of the P(VDF–TrFE) and TiOPc. In addition, this setup allowed applying a driving voltage with/without visible-light illumination.

Figure 1a shows the detected uniform diffraction rings of the P(VEF–TrFE) piezoelectric thin film. The results indicate that there is no preferred orientation in the semi-crystalline structure of the P(VDF–TrFE) thin film used in this study. Figure 1b illustrates the diffractions of the (110) and (310) planes. Since the repeating unit of PVDF is composed of a carbon back bone with two hydrogen and two fluorine atoms, a net dipole moment is formed, pointing from the relatively electronegative fluorine to the hydrogen.[19] This unique polarization of P(VDF–TrFE) is the source of its piezoelectric properties. The piezoelectric behavior is usually achieved by electric field poling with a high voltage source, as shown in **Figure 2**f and Figure 1b. A detailed procedure of the sample preparation is summarized in Figure 2.

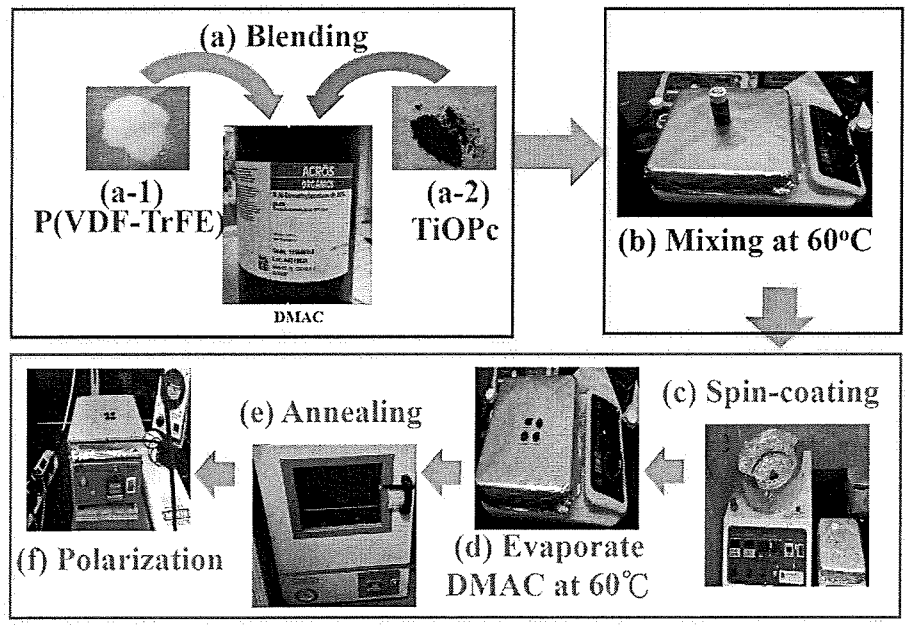

Figure 2. Sample-preparation procedures: a) Blending (a-1) poly(vinylidene fluoride-co-trifluoroethylene) (P(VDF–TrFE)) with (a-2) titanium oxide phthalocyanine (TiOPc) powders. b) Mixing the composite at 60 °C. c) Spin-coating the composed film on a PET plate with an ITO electrode. d) Heating the sample to evaporate dimethylacetamide (DMAc) solvent. e) Annealing the sample in a 100 °C vacuum oven for six hours. f) Polarizing the samples.

© 2015 WILEY-VCH Verlag GmbH & Co. KGaA, Weinheim

ADVANCED MATERIALS
www.advmat.de
www.MaterialsViews.com

The application of X-ray diffraction to investigate the relationship between the microstructure and the properties of P(VDF–TrFE) thin films was reported by Jung et al.[20] Following the same approach, we present, for the first time, a study on the lattice evolution of *a* and *b* parameters based on the measured d-spacing of (110) and (310) planes coupled with two piezoelectric coefficients, d_{33} and d_{31}, which have been well characterized by Zeng et al.[21] We assumed that the responses of the polarized *b*-axis of the structure and its orthogonal *a*-axis have a ratio of d_{33} and d_{31} when subjected to the applied field.

The evolution of lattice- and bulk-strains subjected to an electrical field for the P(VDF–TrFE) polymer blended with and without TiOPc nanoparticles is shown in **Figure 3**a and 3b, respectively. Both systems show that the polarized *b*-axis lattice strain (circles) elongated parallel to the bulk d_{33} strain (squares). The perpendicular *a*-axis lattice strain (up triangles) compresses accordingly. In Figure 3b, the down triangles show the measured lattice strains of TiOPc, which suggest that there is no direct correlation between the applied electric field and TiOPc. In Figure 3c, the fluctuated peak-width evolution of the P(VDF–TrFE) evidences that there is no microstructure development, such as aggregation or defects formation, under application of a driving voltage of up to 600 V.

To further investigate the effect of visible light illumination, the same specimens were first measured without light illumination and then with light illumination under identical experimental conditions. The direct comparisons are shown in **Figure 4**a for P(VDF–TrFE) without TiOPc and Figure 4b for P(VDF–TrFE) with TiOPc, respectively. In Figure 4, the

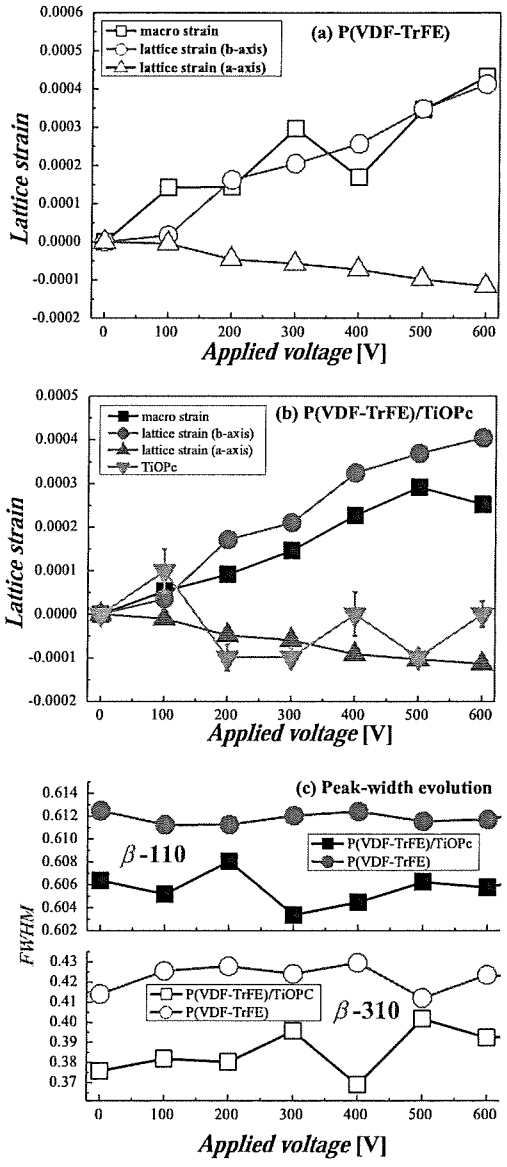

Figure 3. a) Macro- (open squares), *b*-axis-lattice (open circles), and *a*-axis-lattice (open triangles) strain evolution of the P(VDF–TrFE) as function of applied voltage (V). b) Macro- (filled squares), *b*-axis-lattice (filled circles), *a*-axis-lattice (filled triangles), and TiOPc-lattice (filled triangles) strain evolution of the P(VDF–TrFE)/TiOPc as function of the applied voltage. c) Upper panel: Full-width-at-half-maximum (FWHM) evolution of the *b*–phase diffraction peaks (110) as function of the applied voltage as (filled circles) for P(VDF–TrFE) and (filled squares) for P(VDF–TrFE)/TiOPc, respectively. Bottom panel: Similarly, full-width-at-half-maximum (FWHM) evolution of the b–phase diffraction peaks (310) as function of the applied voltage as (open circles) for P(VDF–TrFE) and (open squares) for P(VDF–TrFE)/TiOPc, respectively.

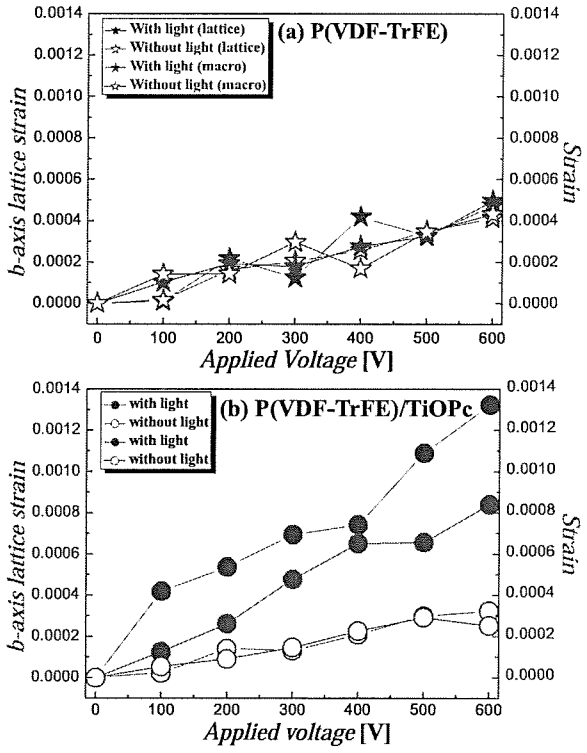

Figure 4. a) Macro-with-light (filled stars), macro-without-light (open stars), *b*-axis-lattice-with-light (filled stars), and *b*-axis-lattice-without-light (open stars) strain evolution of the P(VDF–TrFE) as function of the applied voltage (V). b) Macro-with-light (filled circles), macro-without-light (open circles), *b*-axis-lattice-with-light (filled circles), and *b*-axis-lattice-without-light (open circles) strain evolution of the P(VDF–TrFE)/TiOPc as function of the applied voltage.

© 2015 WILEY-VCH Verlag GmbH & Co. KGaA, Weinheim

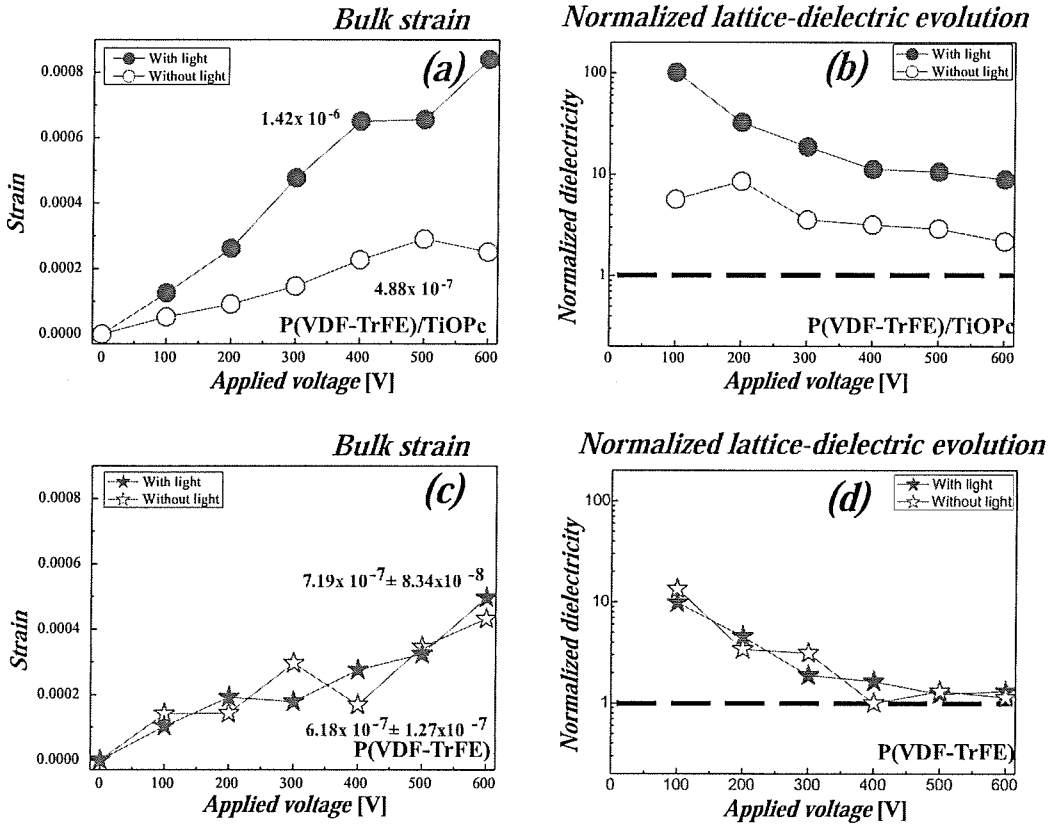

Figure 5. Bulk- and lattice-dielectric responses for P(VDF–TrFE)/TiOPc: a) Bulk-strain (d_{33}) evolution as function of the applied voltage with light (filled circles) and without light (open circles), b) Calculated-lattice-dielectric evolution as function of the applied voltage with light (filled circles) and without light (open circles). Bulk- and lattice-dielectric responses for P(VDF–TrFE): c) Bulk-strain (d_{33}) evolution as function of the applied voltage with light (filled stars) and without light (open stars), d) Calculated-lattice-dielectric evolution as function of the applied voltage with light (filled stars) and without light (open stars).

double *y*-axes show lattice responses on the left and bulk responses on the right, respectively. The blue stars are the *b*-axis lattice strain and the red stars are the macroscopic d_{33} results. The solid and empty stars are data measured with and without illumination, respectively. Qualitatively, in Figure 4a, which shows the samples without TiOPc, both bulk and lattice strains are not influenced by the visible-light illumination. On the other hand, in Figure 4b, there is a significant effect after being subjected to the visible-light illumination at both the lattice and bulk levels. Furthermore, both the bulk and lattice strain of P(VDF–TrFE) without TiOPc are greater than that of P(VDF–TrFE) with TiOPc. The slope of P(VDF–TrFE) without TiOPc is $6.2\times10^{-7}V^{-1}$. This value is greater than the slope of the P(VDF–TrFE) with TiOPc $(4.9\times10^{-7}V^{-1})$. The bulk piezoelectric responses of P(VDF–TrFE) with TiOPc are reduced by the addition of TiOPc nanoparticles, which indicates that it has a relatively weaker piezoelectric effect. However, when this sample was illuminated with light, the bulk piezoelectric response of P(VDF–TrFE) with TiOPc was two times higher than that without light. Finally, the lattice responses shown in Figure 4b (solid versus empty circles) are much larger than that of the bulk responses, d_{33}, (solid circles versus open circles) when subjected to light illumination. This is because the bulk specimen containing the TiOPc shows no piezoelectric effect. The slope of the bulk piezoelectric responses of P(VDF–TrFE) with TiOPc becomes $14.2\times10^{-7}V^{-1}$.

To compare the conventional d_{33} results and the newly resolved lattice responses, we determined the bulk-strain-applied voltage responses and lattice-deduced-dielectric-constant evolution. The results are shown in **Figure 5**. The bulk strain and the lattice-dielectric evolution of P(VDF–TrFE) with TiOPc nanoparticles are plotted in Figure 5a and 5b, respectively. The responses when subjected to light and without light illumination are labeled with solid circles and empty circles. The corresponding results of P(VDF–TrFE) without TiOPc are shown in Figure 5c and 5d, respectively. The slope of the bulk d_{33} versus the applied voltage is also listed in Figure 5a and 5c. Without light illumination, the slope of P(VDF–TrFE) with TiOPc is $4.9\times10^{-7}V^{-1}$, which is less than that of P(VDF–TrFE) without TiOPc $(6.2\times10^{-7}V^{-1})$. However, upon light illumination, the slope of P(VDF–TrFE) with TiOPc becomes $14.2\times10^{-7}V^{-1}$ for the bulk piezoelectric responses, which is about twice as high as than that of P(VDF–TrFE) without TiOPc.

To understand these modulation effects we carried out an experiment to measure visible-light absorbance spectra.[6,12] Unlike the pure P(VDF–TrFE) with weak visible light

© 2015 WILEY-VCH Verlag GmbH & Co. KGaA, Weinheim

absorbance, the P(VDF–TrFE) and TiOPc-blended composite show an expanded absorbance band from the visible-light to infrared regions. The gap between the modulated lowest unoccupied (LUMO) and the highest occupied (HOMO) molecular orbital of the system with TiOPc decreases. Without light illumination, the piezoelectricity mechanism is identical between the systems with and without TiOPc because only P(VDF–TrFE) responds to the applied voltage. However, when the systems are excited by light, the molecular orbitals of P(VDF–TrFE) tuned by TiOPc allow more transfers of the local charges for piezoelectricity.[6,12]

We follow Huang et al.'s method[22] to achieve an effective dielectricity evolution based on the lattice response. Huang et al. reported the following formula[22] to estimate the dielectric value (K):

$$K = \frac{2S \times Y}{E^2 \times \varepsilon_0 \times (1+2\nu)} \quad (1)$$

where ε_0 is vacuum permittivity (8.85×10^{-12} F m^{-1}), Y is the documented modulus of elasticity, E is the applied electrical potential, and ν is Poisson ratio of the system. Both the elastic modulus[23] and Poisson ratio[21] were taken from previous reports. However, unlike the effective dielectric constant defined by Rao and Li,[24] we normalize the dielectricity at lattice level to allow comparisons between our measurements. Figure 5b and 5d were plotted by using Equation (1) with parameters taken from the measured structural-resolved lattice-strain, S, and the applied voltage, E, to plot. It was found that there was a significant visible-light effect (Figure 5b). In contrast, such a photon-illumination effect was not observed in a pure P(VDF–TrFE) material (Figure 5d). In both Figure 5b and 5d, there is a greater lattice-dielectric response at the initial charging stage, after which the lattice-dielectric values decay with the coercive field (E_c), even when the b-axis continues to expand, as shown in Figure 4. Because the denominator of Equation (1) increases as the square of the applied voltages increases, the b axis, as the nominator of Equation (1), only increases linearly. The results shown in Figure 5b and 5d demonstrate that the lattice-dielectric levels can be tuned by adding TiOPc powder as well as by light modulation. Although typical electroactive polymers (EAPs) have averaged dielectric properties at bulk level, Zhang and co-workers have shown that all-organic composite actuator materials may have a high dielectric constant exceeding 50 000, which is due to delocalized charges in a composite blocking the long-range space charge conduction.[25] It has also previously been reported that the interface enhances the dielectricity.[26] Similarly, in the present system, the boundary layers between the PVDF–TrFE matrix and the TiOPc powders could act as an internal boundary layer capacitor resulting in a high lattice-dielectric value in the P(VDF–TrFE) matrix for a brief period, which explains the aforementioned initial-charging peaks shown in Figure 5b and 5d. Since both of our systems show the same behavior for the conditions with (Figure 5b) and without TiOPc (Figure 5d), we hypothesize that a local configurational entropic effect[23,27] might also occur during the initial charging stage. Later on, the system could gradually reach a steady state at higher applied voltage. It is also reported that due to Maxwell–Wagner polarization originating at the insulator–conductor interfaces,[28] the dielectric property of composites can be greatly enhanced, and better than that of the polymer matrix. This enhancement of the dielectric constant can be correlated with the percolation in the system.[29] At higher levels of the applied electric voltage, the dielectric relaxation is practical for interconnected conductive networks.[30] The detailed mechanisms of this transition in our systems and the influence of characteristic lattice evolution on the micromechanics are, however, beyond the scope of this paper.

The three-way piezo-phototronic effect enables interactions that allow coupling of piezoelectricity, photonic excitation, and semiconductor transport. A semi-crystalline polymer, P(VDF–TrFE) (poly(vinylidene fluoride-co-trifluoroethylene)) blended with TiOPc powder, which has excellent sensitivity to visible light, is expected to bridge photo-conductor and piezoelectric actuators. In this study, the real-time synchrotron X-ray diffraction experiments revealed the underlying structural evolution. P(VDF–TrFE) was identified to have an all-trains β-phase (TTTT) conformation. The lattice-strain evolution is proportional to the applied voltage, but the lattice responses with/without light illumination are subject to the presence of the TiOPc effect. The dynamics of the bulk piezoelectric response, d_{33}, are slower than that at lattice level. The effective dielectric values, calculated from the measured lattice strain, gradually reached steady state at 600 V. P(VDF–TrFE) with embedded TiOPc showed a peak in the dielectric value at the initial stage of the applied voltage. These experimental findings allowed us to tune and control the piezopotential-induced strain for bio-related applications, such as lab-on-a-chip systems and wearable electronic systems. With further improvements in the composite fabrication process, such as using different sizes and morphology of the TiOPc particles, the piezo-phototronic effect can be tailored. In view of the flexible soft piezo-phototronics, the presented results demonstrate the potential of this new class of composites for the development of photon-modulated piezoelectric polymer-like materials.

Experimental Section

Sample Preparation: The P(VDF–TrFE) of 70–30 mol% copolymer powder was ordered from PiezoTech S.A. The titanium oxide phthalocyanine (TiOPc, $C_{32}H_{16}N_8OTi$) powder with an absorbance peak of 692 nm was obtained from Sigma-Aldrich Corporation. The solvent for mixing these two materials was dimethylacetamide (DMAC) (Acros). The P(VDF–TrFE) of 70–30 mol% was first dissolved in a DMAC solvent followed by adding TiOPc solutions to form a mixture of 70–30 mol% P(VDF–TrFE) with 10 wt% TiOPc. Then, the P(VDF–TrFE)-TiOPc mixture was stirred continuously for one day to mix the solution thoroughly. The P(VDF–TrFE)-TiOPc thin-film was then spun onto an ITO glass by way of spin coating. TiOPc-coated ITO glass was annealed in a vacuum oven at 100 °C for six hours. The detailed sample preparation procedure is summarized in Figure 2.

Here, the P(VDF–TrFE) of 70–30 mol% copolymer showed the best performance of the systems that we tested.[6,12] There is a first-order transition from a β-phase to a α-PVDF between 40 and 50 °C.[31] In fact, the unit cell of the P(VDF–TrFE) copolymer, i.e., the intermolecular lattice structure, chain packing and dipolar alignment are almost the same as in the case of β-PVDF. The β-content can be enhanced under stretching[32] and poling.[33] Although the ferroelectric phase occurs in the copolymer P(VDF–TrFE) at room temperature without additional electric poling or stretching, the unit cells orientate randomly in the

© 2015 WILEY-VCH Verlag GmbH & Co. KGaA, Weinheim

semi-crystalline polymer, which is similar to the β-phase, and display ferro–paraelectric phase transition before the melting of the crystalline phase.[17]

In Situ Synchrotron X-ray Diffraction Measurements: The in situ X-ray diffraction experiments were carried out at the National Synchrotron Radiation Research Center (NSRRC) at Taiwan. Synchrotron X-ray measurements were carried out in transmission mode; a detailed setup has been reported elsewhere.[34] The advantages of nondestructive scattering/diffraction measurements have been reported for many applications.[35] A complementary bulk piezo-phototronic effect was measured by a d_{33} meter to compare them with experimental results from X-ray diffraction analysis.

Acknowledgements

E.W.H. appreciates the support of Ministry of Science and Technology (MOST) Program 104–2628-E-009–003-MY3 and National Chiao Tung University – Office of Research and Development Program 104W986. EW.H. and his co-workers very much appreciate the beam time and help from the beamlines 01C2 and 13A with Dr. Ming-Tao Lee of the National Synchrotron Radiation Research Center (NSRRC).

Received: July 10, 2015
Revised: August 28, 2015
Published online: October 19, 2015

[1] Z. L. Wang, *Adv. Mater.* **2012**, *24*, 4632.
[2] Q. Yang, X. Guo, W. H. Wang, Y. Zhang, S. Xu, D. H. Lien, Z. L. Wang, *ACS Nano* **2010**, *4*, 6285.
[3] Q. Yang, W. H. Wang, S. Xu, Z. L. Wang, *Nano Lett.* **2011**, *11*, 4012.
[4] C. K. Jeong, J. Lee, S. Han, J. Ryu, G. T. Hwang, D. Y. Park, J. H. Park, S. S. Lee, M. Byun, S. H. Ko, *Adv. Mater.* **2015**, *27*, 2866.
[5] H. C. Shih, C. Y. Lu, W. H. Hsiao, C. T. Lin, C. K. Lee, *Eighth International Conference on Adaptive Structures and Technologies* **1998**, 204.
[6] W.-C. Chang, A.-B. Wang, C.-K. Lee, H.-L. Chen, W.-C. Ko, C.-T. Lin, *Ferroelectrics* **2013**, *446*, 9.
[7] a) Y. Guo, G. Yu, Y. Liu, *Adv. Mater.* **2010**, *22*, 4427; b) S. K. Hwang, I. Bae, R. H. Kim, C. Park, *Adv. Mater.* **2012**, *24*, 5910.
[8] a) T. Sharma, S.-S. Je, B. Gill, J. X. Zhang, *Sens. Actuators A: Phys.* **2012**, *177*, 87; b) M. Bachmann, W. Gordon, S. Weinhold, J. Lando, *J. Appl. Phys.* **1980**, *51*, 5095.
[9] C. A. Nguyen, P. S. Lee, W. A. Yee, X. Lu, M. Srinivasan, S. G. Mhaisalkar, *J. Electrochem. Soc.* **2007**, *154*, G224; b) H.-M. Bao, C.-L. Jia, C.-C. Wang, Q.-D. Shen, C.-Z. Yang, Q. Zhang, *Appl. Phys. Lett.* **2008**, *92*, 042903.
[10] W.-Y. Chang, T.-H. Fang, S.-Y. Liu, Y.-C. Lin, *Mater. Sci. Eng: A* **2008**, *480*, 477.
[11] B. Ameduri, *Chem. Rev.* **2009**, *109*, 6632.
[12] W.-C. Chang, A.-B. Wang, C.-K. Lee, H.-L. Chen, W.-C. Ko, C.-T. Lin, "Development of a photoconductive piezoelectronic material from composite of P (VDF–TrFE) and TiOPc", presented at *2012 European Conference on the Applications of Polar Dielectrics and 2012 International Symp Piezoresponse Force Microscopy and Nanoscale Phenomena in Polar Materials*, July, **2012**.
[13] S. Satapathy, S. Pawar, P. Gupta, K. Varma, *Bull. Mater. Sci.* **2011**, *34*, 727.
[14] *The Applications of Ferroelectric Polymers* (Eds: T. T. Wang, J. M. Herbert, A. M. Glass), Blackie and Son, Glasgow, UK **1988**.
[15] Y. Takahashi, Y. Matsubara, H. Tadokoro, *Macromolecules* **1983**, *16*, 1588.
[16] H. Wang, Q. Zhang, L. Cross, A. Sykes, *J. Appl. Phys.* **1993**, *74*, 3394.
[17] S. Guo, C. Sun, T. Wu, X. Zhao, H. L. Chan, *J. Mater. Sci.* **2007**, *42*, 1184.
[18] K. Omote, H. Ohigashi, K. Koga, *J. Appl. Phys.* **1997**, *81*, 2760.
[19] G. Davis, J. McKinney, M. Broadhurst, S. Roth, *J. Appl. Phys.* **1978**, *49*, 4998.
[20] H. J. Jung, J. Chang, Y. J. Park, S. J. Kang, B. Lotz, J. Huh, C. Park, *Macromolecules* **2009**, *42*, 4148.
[21] R. Zeng, K. W. Kwok, H. L. W. Chan, C. L. Choy, *J. Appl. Phys.* **2002**, *92*, 2674.
[22] C. Huang, Q. M. Zhang, J. Su, *Appl. Phys. Lett.* **2003**, *82*, 3502.
[23] E. Bellet-Amalric, J. F. Legrand, *Eur. Phys. J. B* **1998**, *3*, 225.
[24] N. Rao, J. Y. Li, *Int. J. Solids Struct.* **2004**, *41*, 2995.
[25] Q. M. Zhang, H. Li, M. Poh, F. Xia, Z. Y. Cheng, H. Xu, C. Huang, *Nature* **2002**, *419*, 284.
[26] Y. Li, X. Huang, Z. Hu, P. Jiang, S. Li, T. Tanaka, *ACS Appl. Mater. Interfaces* **2011**, *3*, 4396.
[27] E. W. Huang, D. Yu, J.-W. Yeh, C. Lee, K. An, S.-Y. Tu, *Scripta Mater.* **2015**, *101*, 32.
[28] V. Bobnar, A. Levstik, C. Huang, Q. M. Zhang, *J. Non-Cryst. Solids* **2007**, *353*, 205.
[29] a) V. Panwar, B. Kang, J.-O. Park, S. Park, R. M. Mehra, *Eur. Polym. J.* **2009**, *45*, 1777; b) Y. Shen, Y. Lin, M. Li, C. W. Nan, *Adv. Mater.* **2007**, *19*, 1418; c) M. Vellakkat, A. Kamath, S. Raghu, S. Chapi, D. Hundekal, *Ind. Eng. Chem. Res.* **2014**, *53*, 16873.
[30] L. Li, B. Qing Zhang, X. Ming Chen, *Appl. Phys. Lett.* **2013**, *103*, 192902.
[31] Z.-Y. Cheng, V. Bharti, T.-B. Xu, H. Xu, T. Mai, Q. Zhang, *Sens. Actuators A: Phys.* **2001**, *90*, 138.
[32] H. Guo, Y. Zhang, F. Xue, Z. Cai, Y. Shang, J. Li, Y. Chen, Z. Wu, S. Jiang, *Cryst. Eng. Comm.* **2013**, *15*, 1597.
[33] S. Oh, Y. Kim, Y. Y. Choi, D. Kim, H. Choi, K. No, *Adv. Mater.* **2012**, *24*, 5708.
[34] E. W. Huang, J. Qiao, B. Winiarski, W.-J. Lee, M. Scheel, C.-P. Chuang, P. K. Liaw, Y.-C. Lo, Y. Zhang, M. Di Michiel, *Sci. Rep.* **2014**, *4*, 4394.
[35] R.-J. Roe, *Methods of X-ray and Neutron Scattering in Polymer Science*, Oxford University Press, USA **1999**.

© 2015 WILEY-VCH Verlag GmbH & Co. KGaA, Weinheim